

# The abundance pattern of the $\lambda$ Bootis stars. <sup>\*</sup>

U. Heiter<sup>1,2</sup>

<sup>1</sup> Institute for Astronomy (IfA), University of Vienna, Türkenschanzstrasse 17, A-1180 Vienna

<sup>2</sup> Department of Astronomy, Case Western Reserve University,  
10900 Euclid Avenue, Cleveland, OH 44106-7215, USA  
email: ulrike@fafnir.astr.cwru.edu

Received ; accepted

**Abstract.** Within a project to investigate the properties of  $\lambda$  Bootis stars, we report on their abundance pattern. High resolution spectra have been obtained for a total of twelve candidate  $\lambda$  Bootis stars, four of them being contained in spectroscopic binary systems, and detailed abundance analyses have been performed. All program stars show a characteristic  $\lambda$  Bootis abundance pattern (deficient heavy elements and solar abundant light elements) and an enhanced abundance of Na. This work raises the fraction of  $\lambda$  Bootis stars with known abundances to 50 %. The resulting abundances complemented by literature data are used to construct a “mean  $\lambda$  Bootis abundance pattern”, which exhibits, apart from general underabundances of heavy elements ( $\approx -1$  dex) and solar abundances of C, N, O, Na and S, a star-to-star scatter which is up to twice as large as for a comparable sample of normal stars.

**Key words.** stars: abundances – stars: atmospheres – binaries: spectroscopic – stars: chemically peculiar – stars: early-type

## 1. Introduction

$\lambda$  Bootis stars are defined as Population I A- to F-type stars, which are metal-poor but exhibit nearly solar element abundances for C, N, O and S (e.g. Hauck & Slettebak 1983; Abt 1984; Gray 1997; Paunzen 2000). A historical review of studies dealing with these stars, as well as extensive work on several aspects regarding the  $\lambda$  Bootis group, like spectral classification, photometry, ultraviolet and infrared fluxes, space motions, binarity and theoretical considerations, can be found in Paunzen (2000).

From the definition above it is obvious that the chemical composition of the atmospheres of  $\lambda$  Bootis stars represents the most important property for the characterization of this group of stars. At the beginning of this project, few abundance determinations for  $\lambda$  Bootis stars existed in the literature (see Sect. 4). It was not possible to make a firm conclusion about “the abundance pattern” of the  $\lambda$  Bootis stars, in particular because only a part of the parameter space occupied by current lists of  $\lambda$  Bootis candidates was covered by abundance analyses.

A detailed knowledge of the common abundance pattern, if existent, and of the variation of abundances of

individual elements with stellar parameters is the key to understanding the astrophysical processes generating the properties of the  $\lambda$  Bootis group. Therefore the determination of abundances for as many elements as possible for preferably all members of this group (where the membership assignment is based on classification spectroscopy) is regarded as a main goal of this investigation. Together with all abundance analyses found in the literature, the proportion of  $\lambda$  Bootis stars with known abundances, based on the list of  $\lambda$  Bootis stars given by Paunzen (2000), amounts now to about 50%, which allows to draw conclusions on the abundance pattern of the  $\lambda$  Bootis stars as a group. A statistical investigation of the  $\lambda$  Bootis parameters and a comparison with other groups of stars and the interstellar medium will be the topic of a subsequent paper.

## 2. Observations and analysis

High resolution and classification resolution spectra with high signal to noise have been obtained at various sites as listed in Table 1. Fig. 1 shows a part of the high resolution spectra of two stars with the most similar atmospheric parameters (see Sect. 3) obtained with two different instruments. They have been reduced with the `ccdred` and

Send offprint requests to: U. Heiter

<sup>\*</sup> Based on observations obtained at the Osservatorio Astronomico di Padua-Asiago, OPD/LNA, KPNO and DSO

**Table 1.** Observations used in this work. The last three columns give the observed wavelength range ( $\lambda$ ), the resolving power (R), and the mean continuum signal to noise ratio determined from the reduced spectra.

HD	Observatory / Telescope	Date	Observer	$\lambda$ [Å]	R	S/N
74873, 84948, 101108, 106223, 110411	Asiago (Italy) / 1.8 m	3–1995	U. Heiter, E. Paunzen	4000–5700	20000	150, 250
84948, 171948		2–1997		4500–7200		200
107233, 142703, 168740, 170680	OPD/LNA (Brazil) / 1.6 m	6–1995	E. Paunzen	3900–4900	22000	150, 200, 230
106223	KPNO (Arizona) / 1.5 m	4–1998	M. Weber	4240–4570	24000	200
74873, 101108, 170680	DSO (N. Carolina) / 0.8 m	1995	R.O. Gray	4000–4450	2200	300, 150, 400
106223	OHP (France) / 1.93 m	1995	E. Paunzen,	4000–4450	1200	300
110411	Asiago (Italy) / 1.8 m	1995	U. Heiter	4000–4450	1100	350
107233, 142703	OPD/LNA (Brazil) / 1.6 m	1995	E. Paunzen	4000–4450	2200	200, 350

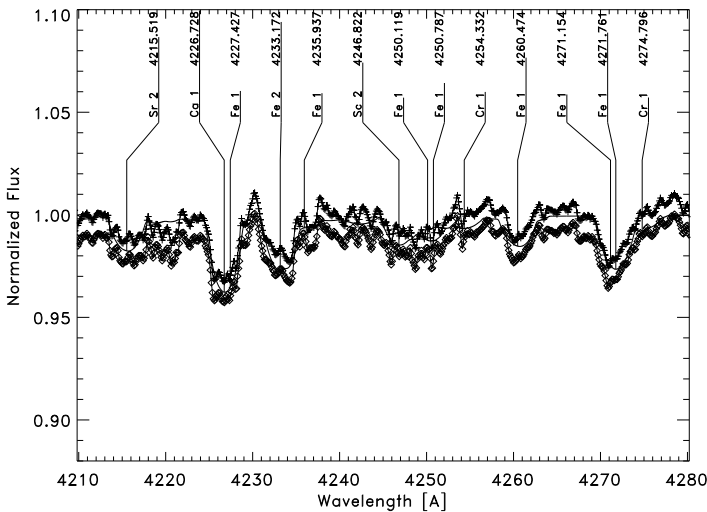


**Fig. 2.** Section of the spectrum of HD 110411 with the continuum of the observed spectrum raised (pluses) and lowered (diamonds) by 0.5%. This seems to be the maximum deviation from the “true” continuum as a comparison with the calculated spectrum (solid line) shows. For better visibility, the observations have been smoothed with a boxcar average using a width of 5 pixels. The flux scale is the same as in the other figures.

*echelle* packages of NOAO IRAF following Willmarth & Barnes (1994).

Particular care has been devoted to the normalization of the spectra to the continuum, which is in general rather difficult for broad lined stars. But in the case of metal poor stars as examined here, the problem is not as serious, because their spectra show sufficiently few lines, so that there are enough continuum sections in between for every echelle order. The interactive curve fitting tool, ICFIT, within IRAF is a convenient help in performing this task. A cubic spline is fit to the data points contained in one echelle order, iteratively excluding those points from the fit whose residuals are greater than the noise level of the observations. The normalized observed spectra were compared to synthetic spectra to check if the chosen continuum sections are devoid of spectral lines. Our experience with VALD based on analyses of stars with a wide range

of metallicities justifies the assumption that these sections indeed do not contain any unknown significant spectral lines.

The error introduced by deviations of the fit from the real continuum level influences mostly the abundances of elements for which only few lines can be used. When using many lines distributed over a large wavelength range for the abundance determination of an element, the continuum placement error is assumed to be negligible compared to the scatter of the “line” abundances (see below) from which the abundance error has been determined. The spectrum of HD 110411 (one of the broadest lined stars) has been raised and lowered by 0.5%, which seems to be a maximum for an incorrect continuum fit (see Fig. 2). The errors resulting from such a displaced continuum amount to 0.1 dex for C, Ca and Ti, and 0.2 dex for Mg and Sr for HD 110411. They have been obtained by dividing the abundance differences of several elements relative to our final values by the square root of the number of lines contained in separate orders.

The procedure of the abundance analysis which has been established in the Vienna working group was described in detail for example by Gelbmann et al. (1997) and Heiter et al. (1998), and is summarized in Heiter (2000). Model atmospheres have been computed with the ATLAS9 program (Kurucz 1993a), but using the CM model (Canuto & Mazzitelli 1991) for the treatment of convection. The Rosseland opacities and the opacity distribution functions (ODFs) have been taken from Kurucz (1993a,b). For a discussion of different convection models and their usefulness for the abundance analysis of  $\lambda$  Bootis stars as well as ODFs calculated for the  $\lambda$  Bootis abundance pattern see Heiter et al. (1998). Synthetic spectra have been calculated with the programs SYNTH and ROTATE (Piskunov 1992), using  $\log g f$  values and further atomic data extracted from the Vienna atomic line database (VALD), which contains the most recent laboratory data (Kupka et al. 1999), and new calculations of van der Waals damping constants (Barklem et al. 2000a).

The physics used in the SYNTH program are the same as that described in Valenti & Piskunov (1996). It includes sophisticated H-line treatment (Barklem



**Table 2.** Examples for the relative change of equivalent width ( $\Delta W$ ) of iron lines when changing the abundance by 0.4 dex. Also given are the wavelength  $\lambda$ , the ionisation stage, the lower excitation potential  $E_{\text{low}}$  and the effective Landé factor  $g_{\text{eff}}$ . Blends where one or two lines are marked with a bullet have been selected for analysis, using the atomic parameters of the marked lines for the atmospheric parameter tests.

$\lambda$ [Å]	Ion	$E_{\text{low}}$ [eV]	$g_{\text{eff}}$	$\Delta W$ [%]
4062.441	1	2.845	1.69	42
4063.276	1	3.368	1.15	25
4063.594	1	1.557	1.09	30
4063.627	1	4.103	1.44	0
4064.450	1	1.557	0.34	3
4135.271	1	3.397	1.59	5
4135.755	1	4.191	1.50	2
4136.521	1	3.368	1.35	12
•4136.998	1	3.415	1.13	73
4137.420	1	4.283	1.24	8
•4187.039	1	2.449	1.48	47
4187.587	1	3.430	1.33	7
4187.617	1	3.640	1.10	0
•4187.795	1	2.425	1.47	46
4582.835	2	2.844	1.63	31
4582.940	1	2.845	1.44	0
•4583.837	2	2.807	1.14	63
4583.999	2	2.704	2.06	4
4584.715	1	3.603	1.66	1

blends of iron lines with equal ionisation stage considered for the analysis of HD 106223 are listed in Table 2. The relative difference in equivalent width of each blend component has been calculated for synthetic spectra with an iron abundance difference of 0.4 dex. Blends have been regarded as useful if the contribution to the equivalent width change of all but one component was less than 50% or if two components equally contributing to equivalent width changes had similar atomic parameters (equal sensitivity to  $T_{\text{eff}}$ ,  $\log g$  and  $v_{\text{micro}}$ ). The atomic data for these, a blend dominating components, have been used in the trend analysis.

### 3. Program stars and results

The program stars examined in this work, except for the two spectroscopic binary systems HD 84948 and HD 171948, are listed in Table 3 along with their characteristics found in the literature. Calculated spectra of two stars are shown in Fig. 1 with the corresponding observations. The final parameters used for the analyses are listed in Table 4.

These spectroscopically determined atmospheric parameters do not differ significantly from the photometrically derived ones except for HD 106223 and HD 107233, for which higher and lower  $\log g$  values, respectively, resulted in more consistent line abundances. The best-fit atmospheric parameters are uncertain by up to 400 K for

**Table 3.** Program stars and their characteristics, excluding the spectroscopic binary systems. Columns 3 and 4 indicate if the depression centered at 1600Å is present and if the C/Al equivalent width ratio measured from IUE spectra is enhanced, as is typical for  $\lambda$  Bootis stars (Faraggiana et al. 1990; Solano & Paunzen 1998), and column 5 shows if the IR spectral properties support the  $\lambda$  Bootis classification (Andrillat et al. 1995).

HD	Spectral type	1600Å	C/Al	IR
74873	kA0.5hA5mA0.5 V $\lambda$ Boo <sup>1</sup>			
101108	A3 IV-V ( $\lambda$ Boo) <sup>2</sup>	yes	no	yes
106223	kA3hF3mA3 V $\lambda$ Boo <sup>2</sup>			yes
107233	kA2hF1mA2 V $\lambda$ Boo <sup>2</sup>			
110411	A0 Va ( $\lambda$ Boo) <sup>3</sup>	yes	yes	yes
142703	kA1hF0mA1 Va $\lambda$ Boo <sup>4</sup>		yes	
168740	hA7mA2 V $\lambda$ Boo <sup>2</sup>			
170680	A0 Van ( $\lambda$ Boo) <sup>5</sup>		yes	

<sup>1</sup> Paunzen & Gray (1997), <sup>2</sup> Paunzen (2000),

<sup>3</sup> Gray (1988), <sup>4</sup> Gray (1991), <sup>5</sup> Gray & Garrison (1987)

$T_{\text{eff}}$ , 0.4 for  $\log g$  and 0.5  $\text{km s}^{-1}$  for  $v_{\text{micro}}$ , which has been estimated from the standard error of the gradient of the linear fit between the atomic parameters determining the sensitivity of the lines to the respective atmospheric parameters (see Sect. 2). The error of  $v \cdot \sin i$  has been estimated from line profile fits to be 10  $\text{km s}^{-1}$ .

An additional check of the parameters can be obtained from  $H_{\beta}$ ,  $H_{\gamma}$  and  $H_{\delta}$  lines, which unfortunately are distributed over several orders in the echelle spectra. This fact and their broad wings makes it very difficult to normalize these regions to the continuum. Fortunately, classification resolution spectra were available for most of the investigated stars (Paunzen 2000), allowing to estimate the continuum flux level for  $H_{\gamma}$  and  $H_{\delta}$  lines fairly well (Fig. 3).

The mean element abundances of all program stars are given in Table 5. Formal errors calculated from the line abundances are given in parentheses in units of the last significant digit and are representative for the quality of the observational data. Other error sources have to be considered additionally, like errors in  $T_{\text{eff}}$  and  $\log g$ , which would change the element abundances, but increase the scatter in the line abundances for the individual elements. These changes depend largely on the chosen model atmosphere parameters and not on the peculiarity of the investigated stars. Values which are typical for the parameter space we are investigating can be found for the  $\lambda$  Bootis star  $\pi^1$  Ori ( $T_{\text{eff}}=8750$  K,  $\log g=4.0$ ) in Venn & Lambert (1990) and are corroborated by our own experience. We have repeated the abundance analysis for HD 168740 focussing on Fe, which is most suitable for this sort of test because of the relatively large number of unblended lines with well-known atomic parameters in two ionization stages. Decreasing the effective temperature by 600 K decreases the Fe abundance by 0.3 dex, but increases the rms deviation of the line abundances from 0.15

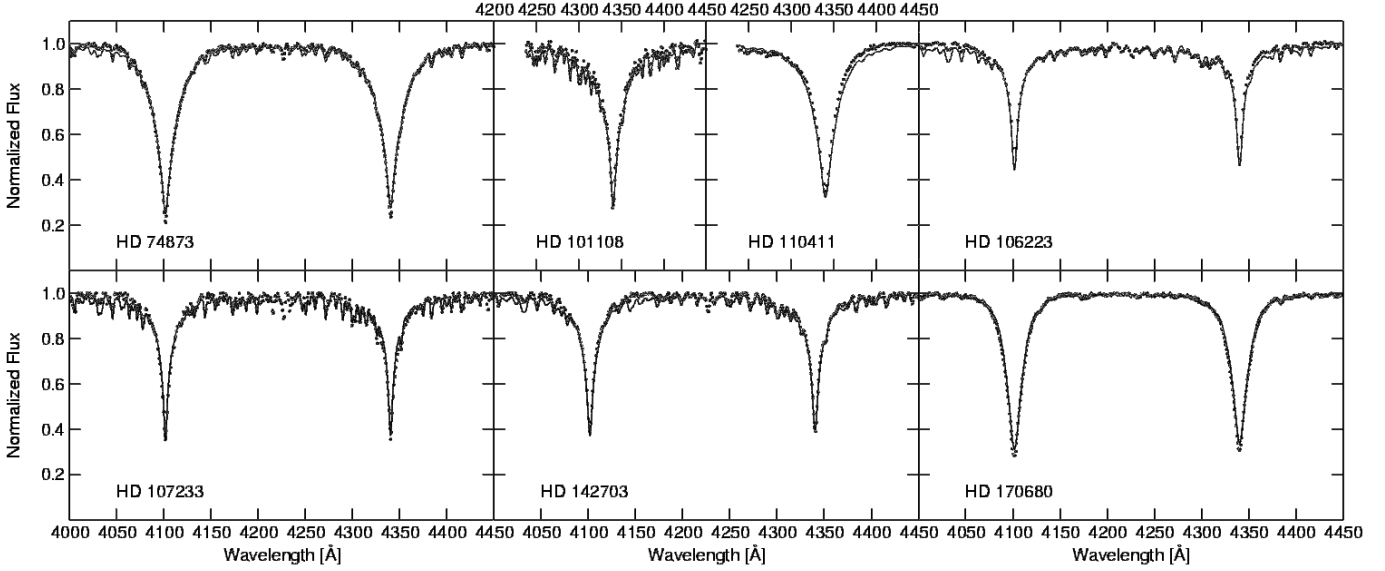


**Fig. 3.** Classification resolution hydrogen line profiles of the program stars. Dots: Observations; Lines: Calculations with parameters as in Table 4, except for HD 74873 ( $\log g=4.3$ ) and HD 106223 ( $T_{\text{eff}}=6800$  K). The characteristics of the observations are given in Table 1.

**Table 4.** Best-fit atmospheric parameters of the program stars.  $[M/H]$  refers to the abundances scale of the ODFs.

HD	$T_{\text{eff}}$ [K]	$\log g$ [log cm s <sup>-2</sup> ]	$v_{\text{micro}}$ [km s <sup>-1</sup> ]	$[M/H]$	$v \cdot \sin i$ [km s <sup>-1</sup> ]
74873	8900	4.6	3.0	-1.0	130
84948A*	6600	3.3	3.5	-1.0	45
84948B*	6800	3.5	3.5	-1.0	55
101108	7900	4.1	3.0	-1.0	90
106223	7000	4.3	3.0	-1.5	100
107233	6800	3.5	3.0	-1.5	80
110411	9200	4.6	3.0	-1.0	150
142703	7000	3.7	3.0	-1.5	100
168740	7900	3.5	3.0	-1.0	130
170680	10000	4.1	2.0	-0.5	200
171948*	9000	4.0	2.0	-1.5	15/10**

\* from Paunzen et al. (1998), \*\* A/B

to 0.24. Increasing the  $\log g$  value by 0.6 dex increases the Fe abundance only by 0.02 dex but increases the rms deviation of the line abundances to 0.19. Uncertainties arising from the continuum fit have been discussed in Sect. 2. The abundances of the neutral and singly ionized elements agree within the observational error limits, indicating a properly chosen atmosphere.

For HD 84948 and HD 171948 the results of the analysis of Paunzen et al. (1998) have been confirmed and extended by using the IDL program BROTE written by O.P. Kochukhov (private communication). Within the error limits the two components of HD 171948 have the same abundances and are therefore listed only once in Table 5b.

In the following, comments on the results of the individual stars are given.

**HD 74873:** The projected rotational velocity of  $130 \text{ km s}^{-1}$  derived from the high resolution spectra corresponds to the similarly high values found for many other  $\lambda$  Bootis stars. It is somewhat higher than the value given in the catalogue of Uesugi & Fukuda (1982) and contradicts the value of  $10 \text{ km s}^{-1}$  given by Abt & Morrell (1995). Thus the star has to be rejected from the (small) list of possibly slowly rotating  $\lambda$  Bootis stars. Abundances for 12 elements could be determined. The underabundances of the heavier elements lie in the range of  $-0.5$  to  $-1$  dex, except for Ni, which seems to be almost solar abundant. The three lighter elements show solar (O) or  $+0.5$  dex higher (C, Na) abundances.

**HD 84948:** For this spectroscopic binary system, abundances for 5 additional heavy elements have been determined, using the same parameters as Paunzen et al. (1998). The two stars belong to the small number of  $\lambda$  Bootis stars for which Zn abundances could be derived. At least for HD 84948 A, Zn is as deficient as the other heavy elements. This is contradictory to the prediction of accretion theory that Zn should resemble the abundances of the light elements (C, N, O, S) because of its similarly low condensation temperature (van Winckel et al. 1992). The same has been found already for HD 84123 (Heiter et al. 1998). Note that the abundance of Y is the highest found for all heavy elements in both stars.

**HD 101108:** Abundances for 14 elements could be determined for this star, as well as an upper limit for the abundance of N. The resulting abundance pattern is typical for  $\lambda$  Bootis stars, with a solar C abundance and a wide range of underabundances (up to  $-1$  dex) for the heavy elements. As in the previous two stars, Y shows the highest abundance of all heavy elements, namely a solar one. The abundance ratio of Al to C seems to contradict the results of the UV measurements presented in Table 3, but

as the Al abundance is based on only one line, its value remains questionable.

*HD 106223*: Element abundances for HD 106223 have been derived already 40 years ago by Burbidge & Burbidge (1956) within their examination of “Five Stars which Show some of the Characteristics of Population II”. A direct comparison to the results of the present work is not possible, because of the different method (curve of growth analysis) and effective temperatures used by them. Furthermore, the abundances are listed relative to 95 Leo, which most probably has non-solar composition (Renson et al. 1991; Abt & Morrell 1995). However, the abundances they derived for HD 106223 are lower than that of HD 84123 (Heiter et al. 1998), but higher than that of  $\lambda$  Boo (Venn & Lambert 1990), which is consistent with the results of the present work. Interestingly, four of the five stars included in the above mentioned work have been assigned to the  $\lambda$  Bootis group later on. The 15 element abundances determined for HD 106223 are characteristic for  $\lambda$  Bootis stars – a slightly higher than solar C abundance and a  $-1.5$  dex mean underabundance of heavy elements. Zn shows a higher than average abundance but not a solar one, and the Y abundance is remarkably high again, although it is based on only one spectral line.

*HD 107233*: The rotational velocity of this star has been determined for the first time in the present work and turned out to have a value typical for  $\lambda$  Bootis stars ( $v \cdot \sin i = 80 \text{ km s}^{-1}$ ). The derived abundances confirm the classification of HD 107233 as a  $\lambda$  Bootis star. C is only slightly deficient whereas the heavy elements are on the average underabundant by  $-1.4$  dex, with an enhancement of Mg and Y and a deficiency of Al relative to Fe.

*HD 110411*: This star has already been analysed by Stürenburg (1993), who gives abundances for only three elements (Ca, Fe and Sr), which are all equally underabundant by  $-1.0$  dex. This result compares well to the new abundance determinations ( $-0.7$ ,  $-1.0$  and  $-1.2$  dex, respectively), if the errors and small differences in the atmospheric parameters (Stürenburg used 8970 K, 4.36 and  $175 \text{ km s}^{-1}$  for  $T_{\text{eff}}$ ,  $\log g$  and  $v \cdot \sin i$ , respectively) are taken into account. Abundances for 6 additional elements are given here, because a much larger wavelength range could be examined in the present work. Of these, the C abundance of  $+0.1$  dex and the (admittedly uncertain) O abundance of  $+0.4$  dex are of particular interest, confirming the  $\lambda$  Bootis character previously attributed to this star due to the properties of its UV spectrum. Further attention should be given to Mg and Si, which seem to be less deficient than the other heavy elements.

*HD 142703*: The C abundance determined in the present work can be compared with the analysis of Paunzen et al. (1999b), which is based on near-IR spectra and non-LTE calculations. Their work resulted in a C abundance of  $-0.5$  dex, which is 0.4 dex lower than the abundance obtained here. This difference can only in part be attributed to the lower  $v \cdot \sin i$  of  $75 \text{ km s}^{-1}$  used by Paunzen et al. (1999b). As another source for the discrepancy, the use of different sets of atomic data was suspected, be-

cause the analysis for this star was made at earlier times than the near-IR analysis, with the then available VALD-1 data (Piskunov et al. 1995). But a comparison of the old and new atomic data for the lines used showed that the differences are very small and would cause uniformly distributed positive and negative shifts in the line abundances. This provides additional indication for an inconsistency of abundances derived from optical and near-IR spectra, as has already been realized by Paunzen et al. (1999b) from a comparison of their results with that of Stürenburg (1993). The Mg, Cr, Fe and Sr abundances agree well with the results of North et al. (1994a,b), if only the spectral lines used in common are regarded. The abundance pattern of HD 142703 is consistent with its  $\lambda$  Bootis classification with underabundances of heavy elements ranging from  $-1$  to  $-1.5$  dex. The  $\lambda$  Bootis character is confirmed by the O abundance of  $-0.1$  dex (Paunzen et al. 1999b). An estimation for the upper limits of the S and Zn abundances has been made, which indicates that these elements are not solar abundant.

*HD 168740*: The Mg, Cr, Fe and Sr abundances determined from the common spectral lines are again similar to that of North et al. (1994a,b), although they used a lower  $v \cdot \sin i$  of  $90 \text{ km s}^{-1}$ . In total, abundances could be determined for eight heavy elements, resulting in underabundances around  $-1$  dex, with Ca and Ba showing about 0.5 dex higher than average abundances. Together with the C and O abundances given by Paunzen et al. (1999b) as  $-0.4$  and  $+0.0$  dex, respectively, HD 168740 exhibits a typical  $\lambda$  Bootis abundance pattern.

*HD 170680*: HD 170680 is the hottest star analysed so far, and it is the fastest rotator of the sample studied here. The  $v \cdot \sin i$  of  $200 \text{ km s}^{-1}$  derived during the analysis confirms the value obtained by Abt & Morrell (1995), as opposed to earlier determinations of  $305 \text{ km s}^{-1}$  (Uesugi & Fukuda 1982). These two properties make an abundance analysis very difficult, because only few suitable lines are seen in the spectrum. On the other hand, the heavy elements are only moderately deficient in this star (up to  $-0.5$  dex) and therefore it was possible to determine rather accurate abundances for four elements. Together with the solar C and O abundances (Paunzen et al. 1999b) they form a mild  $\lambda$  Bootis abundance pattern.

*HD 171948*: The 1997 observations obtained for this spectroscopic binary (SB) system had a lower resolution than the previous observations which lead to the discovery of the binarity. Therefore, in the new spectra, the corresponding lines of the two components were combined in blends, leaving about half of each profile distinguishable. The known  $v \cdot \sin i$  values (in particular their being not equal) and atmospheric parameters (Paunzen et al. 1998) made it possible to determine the radial velocity difference of the two SB components in the new observations, which was only half the value of 1996. Consequently, the observed spectra could be reproduced by synthetic ones, using the parameters and abundances determined previously. Additionally, upper limits and estimates for abundances of other elements could be derived, in particular

**Table 5.** Abundances of the program stars. For each element  $X$  the value  $\log \left( \frac{N_X}{N_{\text{tot}}} \right) - \log \left( \frac{N_X}{N_{\text{tot}}} \right)_{\odot}$  is given, where the solar abundances are taken from Grevesse et al. (1996). The columns containing the numbers of lines per element for two ionisation stages are labeled N. Errors in parentheses are standard errors of the mean line abundances and are given in units of the last significant digit. No errors are given when only one line has been used.

Element	N	74873	N	84948 A	N	84948 B	N	101108	N	106223
C	8/0	+0.6(1)					7/0	+0.1(1)	6/0	+0.3(1)
N							1/0	< +0.7		
O	1/0	+0.0								
Na	1/0	+0.5	2/0	-0.3(4)	2/0	+0.0(3)				
Mg	4/1	-0.9(1)	5/1	-1.2(5)	7/1	-1.0(4)	6/1	-0.3(1)	2/1	-1.7(1)
Al	1/0	-1.1					1/0	-0.9	1/0	-2.1
Si			0/2	-0.8(4)	0/2	-0.6(5)	1/1	-0.5(3)	1/0	-1.7
Ca	1/1	-0.7(1)	11/0	-1.3(5)	9/0	-0.8(4)	7/0	-0.6(1)	4/1	-1.9(1)
Sc	0/1	-0.4	0/6	-1.4(4)	0/6	-0.7(5)	0/3	-0.6(2)	0/2	-2.1(3)
Ti	0/6	-0.9(1)	1/11	-1.4(3)	1/20	-0.6(4)	0/17	-0.3(1)	0/11	-1.6(1)
Cr	2/1	-0.3(2)	7/6	-1.1(4)	4/6	-0.9(5)	4/7	-0.6(1)	4/2	-1.7(1)
Mn							6/0	-0.4(1)	5/0	-1.7(2)
Fe	14/8	-0.6(1)	43/11	-1.1(3)	47/9	-0.9(2)	36/10	-0.60(4)	35/11	-1.44(4)
Ni	1/0	-0.2	4/0	-0.6(4)	4/0	-0.6(4)	6/0	-0.2(1)	5/0	-1.1(1)
Zn	1/0	< +0.9	2/0	-0.9(4)	1/0	-0.4			2/0	-0.8(1)
Sr	0/2	-0.9(4)	0/2	-1.3(5)	0/2	-0.8(4)	0/2	-0.7(2)	0/1	-1.7
Y			0/3	-0.5(4)	0/2	-0.2(4)	0/3	+0.0(2)	0/1	-0.5
Ba			0/4	-1.0(4)	0/2	-0.8(5)	0/2	-0.7(2)	0/2	-1.6(1)

**Table 5.** continued.

Element	N	107233	N	110411	N	142703	N	168740	N	170680	N	171948A/B
C	2/0	-0.3(3)	6/0	+0.1(2)	6/0	-0.1(1)					3/0	< -0.5
N	1/0	< +0.2										
O			1/0	+0.4							2/0	-0.6(4)
Na											5/0	+0.2(4)
Mg	2/1	-0.8(1)	3/1	-0.5(2)	1/1	-1.2(1)	1/1	-0.9(1)	0/2	-0.2(1)	0/1	-2.4
Al	1/0	-2.2										
Si			0/1	-0.3							0/2	-1.6(4)
S					1/0	< -0.7						
Ca	4/0	-1.4(1)	1/1	-0.7(1)	4/0	-1.2(1)	4/0	-0.6(1)				
Sc	0/1	-1.7	0/1	-1.1	0/1	-1.5	0/2	-1.1(4)				
Ti	0/11	-1.4(1)	0/6	-0.9(1)	0/9	-1.4(1)	0/10	-1.1(1)	0/5	-0.5(1)	0/5	< -3.0
Cr	2/1	-1.5(2)			2/3	-1.39(4)	3/6	-1.1(1)	0/3	-0.4(2)	0/2	-1.8(5)
Mn	4/0	-1.3(1)										
Fe	27/5	-1.40(3)	10/5	-1.0(1)	21/8	-1.52(3)	16/11	-0.89(3)	1/9	-0.4(1)	5/10	-1.6(4)
Co	1/0	-1.0										
Ni					3/0	-0.9(2)						
Zn					2/0	< -0.6						
Sr	0/1	-1.3	0/2	-1.2(2)	0/1	-1.2	0/1	-1.0				
Y	0/2	-0.9(2)										
Zr	0/1	-1.5										
Ba					0/1	-1.5	0/1	-0.5				

for some light elements. Lower limits for the Na abundance have been determined by the fit to the resonance lines  $\lambda\lambda$  5890/6, which yielded LTE abundances of +1.4 and +0.7 dex, respectively. The NLTE effect can amount to -0.8 dex for these lines (Mashonkina et al. 1996). The combination with upper limits given by several very weak lines ( $\lambda\lambda$  4978.5,  $\lambda\lambda$  4982.8,  $\lambda\lambda$  6160.7), results in a solar-like Na abundance, whereas C is deficient by at least 0.5 dex. Oxygen shows an underabundance of -0.6 dex,

which is still high compared to the heavy element abundances. These abundance values are the same for both components within the error limits.

The abundance patterns of all program stars are illustrated in Figs. 4 and 5. These Figures, as well as Table 5, include also the abundances of the spectroscopic binaries already reported in Paunzen et al. (1998).

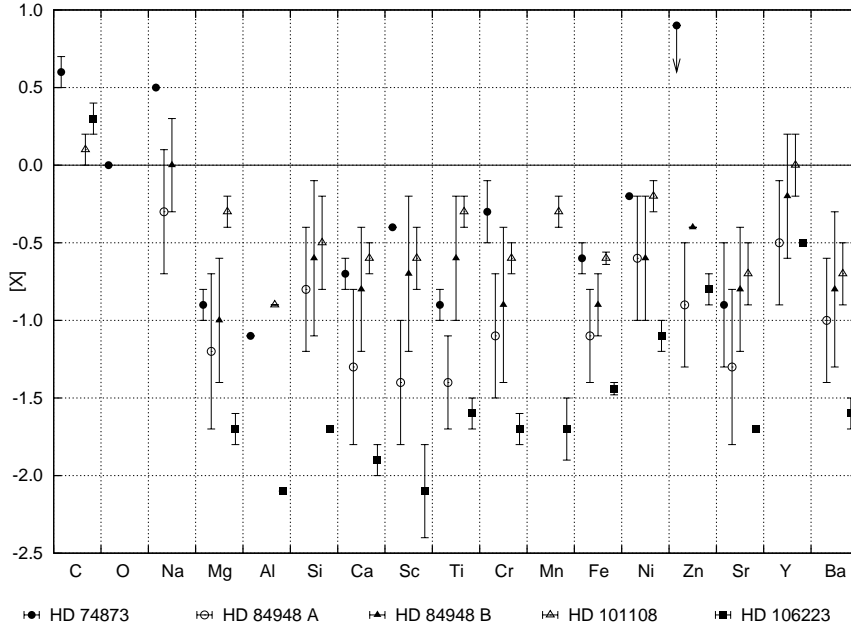


**Fig. 4.** Abundances of the program stars from Table 5 (first five stars). Upper limits are marked by arrows pointing downwards.

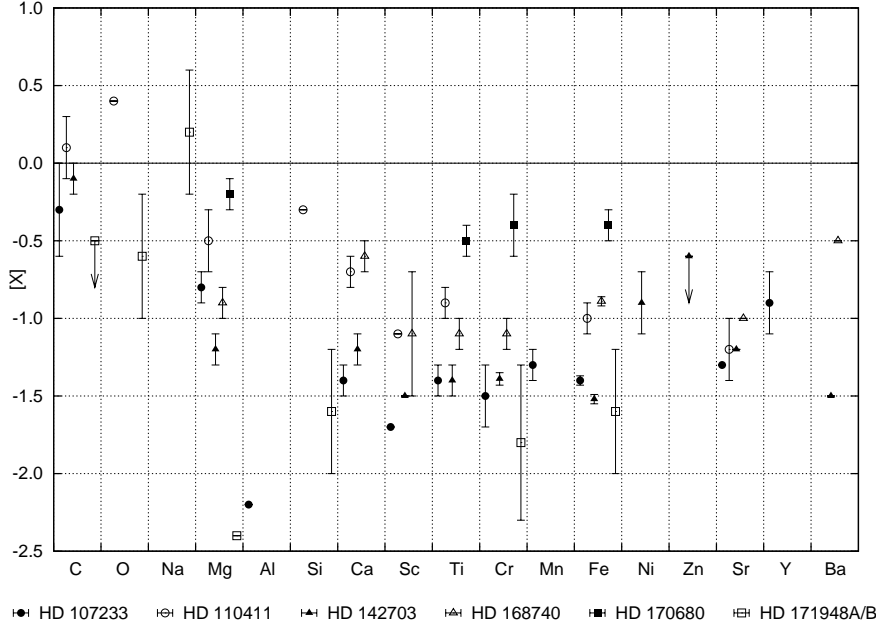


**Fig. 5.** Abundances of the program stars from Table 5 (last six stars).

#### 4. The $\lambda$ Bootis star abundance pattern

Abundances for  $\lambda$  Bootis stars have been taken from the sources listed in Table 6. For the construction of the abundance pattern, abundances determined for the same element by more than one author have been averaged. In a few cases, the abundances differ by more than 0.6 dex and these have been dismissed from the investigation. Also, the abundances derived by Venn & Lambert (1990) for C have been discarded, because they are based on near infrared (NIR) lines. C and O lines in this part of the spectrum have been investigated in more detail by Paunzen et al. (1999b) and their abundances are treated as a separate set, because they found a systematic difference between their results and that of optical abundance anal-

yses (see also Fig. 6). Abundances are available for the following stars whose spectra should be considered composite (Faraggiana & Bonifacio 1999): HD 111786 turned out to be a spectroscopic binary after the abundance analysis was made, and HD 38545 and HD 141851 are visual binaries with separations smaller than  $0.2''$  ( $\Delta m = 0.6$  for HD 38545). Indications for spectroscopic binarity similar to HD 111786 were found for HD 149303 by Paunzen et al. (1999b). The abundances derived for these stars cannot be regarded as reliable, because the influence of the second star has not been taken into account. Therefore they have not been included in the investigations below and are parenthesized in Table 6. The errors of the remaining abundances have been derived from the standard deviation in case of at least three available abundances. From



**Table 6.** References for element abundances determined for  $\lambda$  Bootis stars. A: Adelman (1999), Ch: Chernyshova et al. (1998), H: Heiter et al. (1998) and this work, K: Kamp et al. (2001), M: Martinez et al. (1998), N: North et al. (1994a,b), P: Paunzen et al. (1999a), So: Solano et al. (2001), St: Stürenburg (1993), V: Venn & Lambert (1990). The HD numbers of spectroscopic binaries treated as single stars in the abundance analyses are given in parantheses.

HD	C	N	O	Na	Mg	Al	Si	S	Ca	Sc	Ti	Cr	Mn	Fe	Co	Ni	Zn	Sr	Y	Zr	Ba
319	St			St	St	St	St		St	St	St	St		St				St			St
11413	St				St		St		St	St	St	St		St				St			St
15165	Ch		Ch	Ch	Ch		Ch	Ch	Ch	Ch	Ch	Ch		Ch		Ch					Ch
31295	P,St	K,V	P,V	P,V	P,St, V			K,P, V	P,St, V	P,St	P,St	P,St		P,St, V		P		St,V			P,St
(38545)	St				St		St		St	St	St	St		St				St			St
74873	H		H	H	H	H			H	H	H	H		H		H		H			
75654		K			So			K	So		So	So	So	So							
81290					So				So	So	So	So	So	So							
83041					So				So	So	So			So							
84123	H	H	H	H	H		H	H	H	H	H	H	H	H	H	H	H	H	H	H	H
84948A				H	H		H		H	H	H	H		H		H	H	H	H		H
84948B				H	H		H		H	H	H	H		H		H	H	H	H		H
101108	H				H	H	H		H	H	H	H	H	H		H		H	H		H
105759					M						M	M	M	M							
106223	H				H	H	H		H	H	H	H	H	H		H	H	H	H		H
107233	H				H	H			H	H	H	H	H	H,So	H			H	H	H	
109738														So							
110411	H		H		H		H		H,St	H	H			H,St				H,St			
111005											So			So							
(111786)	St			St	St	St	St		St	St	St	St		St				St			St
125162	P	K,V	P,V	V	P,V		P	K	V	P	P,V	P		P,V		P		V			P
(141851)														N				N		N	
142703	H	K			H,So			K	H	H	H,So	H		H,So		H		H		N	H
(149303)					P						P			P		P					
156954									So		So	So		So							
168740					H		N		H	H	H,So	H		H,So				H		N	H
170680					H						H	H		H							
171948A			H	H	H		H					H		H							
171948B			H	H	H		H					H		H							
183324	H,St	H,K	H	St	H,St	St	St	K	H,St	H	H,St	H,St		H,St				H,St			St
192640	P,St	K,V	A,H, P,V		A,H, P,St, V	A	P,St	K,V	A,H, P,V	A,H	A,H, P,St, V	A,H, P,St	H	A,H, P,St, V		P		A,H, V	A	A	A,H, St
193256	St			St	St		St		St	St	St	St		St				St			St
193281	St	K		St	So,St	St	K		St		St	St		So,St				St			St
198160	St			St	St		St		St		St	St		St				St			St
198161	St			St	St		St		St		St	St		St				St			St
204041	P,St	K	P		P,So, St	St	P,St	K,P	P,St	P,St	P,So, P,St	P,So, P,St		P,So,		P		St			P,St
210111	St			St	So,St	St	St		So,St	St	So,St	So,St		So,St				St			St
221756	P	K	P		P,St		P	K	P	P	P,St	P,St		P,St							St

two available sources, if the two abundances were different, the larger of the two errors given in the references has been taken, and if the two abundances coincided, the smaller of the errors has been taken. In addition to the elements listed in Table 6, abundances of V, Cu, La, Nd and Eu have been derived for one star (Heiter et al. 1998).

Fig. 6 shows the abundance pattern, which results from calculating the mean of the abundances derived for all stars for one particular element. Also shown are the largest and smallest occurring abundances, and the numbers of available abundances per element are given. The mean

abundance values, the standard deviations, as well as the differences of the mean to the maximum and minimum abundances are listed in Table 8. When regarding only the *mean* abundances, the “ $\lambda$  Bootis pattern” is clearly visible, with depleted heavy elements and nearly solar light elements, including Na and S. However, two things are striking within this pattern: First, the difference between abundance determinations of C and O from optical and NIR spectra mentioned above is obvious. Second, the abundance of Zn, which has been found to be non-depleted in the interstellar medium (ISM abundances will be pre-

**Table 7.** Zn I lines analysed in the four  $\lambda$  Bootis stars HD 84123 (1), HD 84948A (2), HD 84948B (3) and HD 106223 (4).

$\lambda$ [Å]	$\log gf$	$E_{\text{low}}$ [eV]	Equivalent width [mÅ]			
			1	2	3	4
4722.153	-0.338	4.030	16	25	30	25
4810.528	-0.137	4.078	22	20		40

sented in Heiter et al. (2001)), is similar to that of the other heavy elements. All available Zn abundances have been determined in the present paper and in Heiter et al. (1998) from the two Zn I lines given in Table 7. We regard these lines to be reliable indicators of the Zn abundance, although Zn I is not the dominant ionization stage in the atmospheres of the studied stars (the fraction of Zn I is about 5 to 15 %). NLTE effects should not play an important role because the analysed lines are rather weak. Furthermore, they have been used by Sneden et al. (1991) for the study of Zn abundances in disk and halo stars with metallicities of  $-3$  to  $-0.2$  dex relative to the Sun and they found the abundances of Zn to be equal to the average of other metals within  $\pm 0.2$  dex. For a sample of normal late-B stars ( $-0.2 \leq [\text{Fe}/\text{H}] \leq 0.2$ ) Smith (1994) has determined Zn abundances from the Zn II resonance lines at 2025 and 2062 Å and also found  $[\text{Zn}/\text{Fe}] = 0 \pm 0.4$ .

Regarding the *minimum* and *maximum* abundances, there is a large scatter in abundance from star to star. More than half of the 15 elements which are *on the average* depleted by  $-0.4$  to  $-1.5$  dex have solar abundance in some stars and Sr and Zr can even be overabundant. Na shows both heavy element like depletions and the largest overabundances of all elements.

To examine the significance of these variations, a similar diagram has been produced for 33 normal A and F dwarfs, which are members of the Hyades cluster and whose effective temperatures and  $v \cdot \sin i$  values lie in the same range as that of the  $\lambda$  Bootis stars, although the sample is biased towards low temperatures (the highest temperature being 8300 K). Their abundances have been taken from Varenne & Monier (1999) and the mean values and abundance ranges are also plotted in Fig. 6. A comparison reveals that for almost all elements the abundance ranges are significantly larger in the  $\lambda$  Bootis stars than in the normal stars, in particular for Na and Mg. They are only comparable to that of the normal stars for Ni, Y and Ba. Additionally, there are differences in the symmetries of the abundance distributions for Na, Si, Sc and Y.

The third set shown in Fig. 6 represents the mean abundances for a smaller and somewhat more inhomogeneous sample of normal B to F stars in the galactic field, which is biased towards high temperatures (more than half of the stars are hotter than 10000 K). They have been extracted from a series of papers (Adelman & Nasson 1980; Adelman 1986, 1987, 1991; Adelman et al. 1991; Adelman & Philip 1992; Adelman 1994; Adelman & Philip 1994;

**Table 8.** Mean abundances of all analysed  $\lambda$  Bootis stars (second column), as well as standard deviations (third column) and difference to highest and lowest abundances (fourth column).

C	0.0	$\pm 0.2$	$+0.6$ $-0.3$	Ti	-0.9	$\pm 0.5$	$+0.8$ $-1.1$
N	-0.1	$\pm 0.3$	$+0.5$ $-0.4$	Cr	-1.0	$\pm 0.4$	$+0.8$ $-0.8$
O	-0.3	$\pm 0.3$	$+0.6$ $-0.4$	Mn	-1.2	$\pm 0.5$	$+0.8$ $-0.9$
Na	0.2	$\pm 0.6$	$+0.8$ $-1.5$	Fe	-1.0	$\pm 0.4$	$+0.8$ $-0.8$
Mg	-1.0	$\pm 0.7$	$+1.1$ $-1.4$	Ni	-0.7	$\pm 0.3$	$+0.5$ $-0.5$
Al	-1.5	$\pm 0.6$	$+0.6$ $-0.8$	Zn	-0.8	$\pm 0.4$	$+0.5$ $-0.5$
Si	-0.8	$\pm 0.5$	$+0.8$ $-0.9$	Sr	-1.0	$\pm 0.6$	$+1.4$ $-1.1$
S	-0.3	$\pm 0.2$	$+0.3$ $-0.4$	Y	-0.6	$\pm 0.4$	$+0.6$ $-0.5$
Ca	-1.0	$\pm 0.4$	$+0.5$ $-1.0$	Zr	-0.4	$\pm 0.7$	$+0.7$ $-1.1$
Sc	-1.1	$\pm 0.4$	$+0.7$ $-1.0$	Ba	-0.8	$\pm 0.4$	$+0.9$ $-0.8$

Adelman 1996; Adelman & Pintado 1997; Caliskan & Adelman 1997; Adelman 1998). On the whole, their abundance pattern looks similar to that of the Hyades stars, although the variations of the *mean* abundances around zero are larger. For C and Ca, the abundance ranges are larger and comparable to that of the  $\lambda$  Bootis stars. On the other hand, the ranges for Sc, Fe and Ba are smaller, but that may be due to the smaller sample size. Note that the mean abundance of Al is the lowest in the normal field stars (almost  $-0.5$  dex) as well as in the  $\lambda$  Bootis stars ( $-1.5$  dex), and that the abundances of S in the normal field stars reach remarkably high values. The largest mean abundance occurs for Zr. It is thus possible that this sample of normal stars is contaminated with mildly chemically peculiar stars.

## 5. Conclusions

We have presented new abundances of up to 15 elements for twelve  $\lambda$  Bootis stars, which include five Y abundances. This element has up to now been studied only for two stars: HD 84123 (Heiter et al. 1998) and 29 Cyg (Adelman 1999). In these stars, the Y abundances are enhanced with respect to that of most other heavy elements. The same is found for all stars presented here. The other heavy elements show underabundances of varying degree, up to about  $-2$  dex, and the light elements C, O and Na appear moderately over- or underabundant, except for HD 171948A/B. In this SB2 system [C] and [O] are less than  $-0.5$  dex, but this is still high compared to the Fe abundance of  $-1.6$  dex.

The results of this work consolidate the membership of all candidate stars to the group of  $\lambda$  Bootis stars,

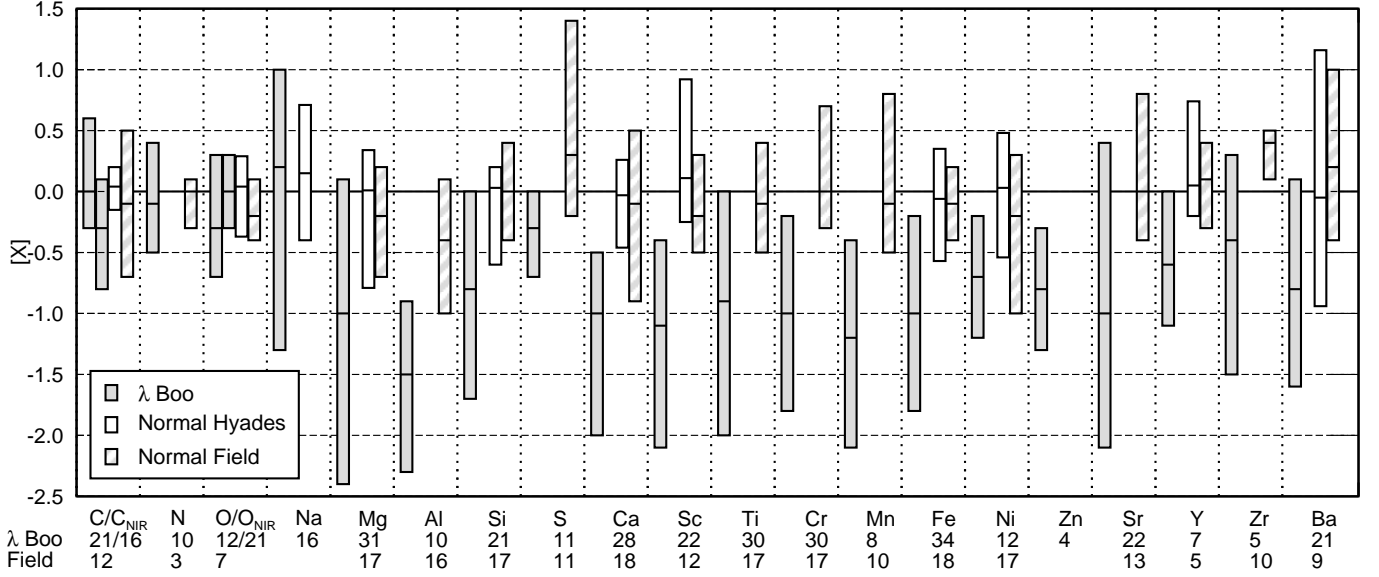


**Fig. 6.** Mean abundances of all analysed  $\lambda$  Bootis stars (middle lines in grey bars), as well as highest and lowest abundances (upper and lower limit of bars). The same for normal stars in the Hyades cluster (white bars) as well as normal field stars (hashed bars). The number of available abundances for the  $\lambda$  Bootis and field stars is given below the element name.

nearly doubling the amount of spectroscopically investigated members of this group of peculiar stars.

In addition, we have collected abundances for 34  $\lambda$  Bootis stars from the literature. They were used to construct a “mean  $\lambda$  Bootis abundance pattern”, which can be described as follows:

- The iron peak elements from Sc to Fe as well as Mg, Si, Ca, Sr and Ba are depleted by about  $-1$  dex relative to the solar chemical composition. The mean abundance of Zn is similarly low, although its condensation temperature is similar to that of S and should prevent the depletion of this element by chemical separation within an accretion scenario.
- Al is slightly more depleted ( $-1.5$  dex) and Ni, Y and Zr are slightly less depleted.
- The abundances of the light elements C, N and O as well as S lie around the solar value, which is not surprising because this is part of the definition of the  $\lambda$  Bootis group. The mean abundance of Na is also solar, but the star-to-star scatter is much larger for this element ( $\pm 1$  dex).
- The star-to-star scatter is twice as large as for a comparable sample of normal stars for all elements except Ba, which means that for more than half of the heavy elements at least one star is included in the sample, for which the abundance of one or more of these elements is solar.

In contrast to the results of Paunzen et al. (1999b), C is on average *more* abundant than O when the abundances are determined from optical lines. The enhanced abundance of Na has been already noted by Stürenburg (1993), who derived a mean abundance of  $+0.6$  dex for his sample of stars, and by Paunzen et al. (1999a).

This description suggests the existence of a separate chemically peculiar group of “ $\lambda$  Bootis stars” with a characteristic abundance pattern. On the other hand, the scatter of abundances for each element indicates that the “ $\lambda$  Bootis group” is rather inhomogeneous. Furthermore, the comparison to normal stars is difficult because the sample of “normal” main sequence stars with known abundances and parameters similar to that of the  $\lambda$  Bootis stars is rather limited.

*Acknowledgements.* The author would like to thank E. Paunzen, M. Weber and R.O. Gray for providing observations and W.W. Weiss for his continuous support and many useful discussions. Thanks go to the referee, K.A. Venn, whose comments have helped to greatly improve the paper. This research was carried out within the working group *Asteroseismology-AMS*, supported by the Fonds zur Förderung der wissenschaftlichen Forschung (project *S 7303-AST*). Use was made of the Simbad database, operated at CDS, Strasbourg, France.

## References

- Abt, H. A. 1984, in *The MK Process and Stellar Classification*, ed. R. F. Garrison, David Dunlop Observatory, Toronto, 340
- Abt, H. A. & Morrell, N. I. 1995, *ApJS*, 99, 135
- Adelman, S. J. 1986, *A&AS*, 64, 173
- 1987, *A&AS*, 67, 353
- 1991, *MNRAS*, 252, 116
- 1994, *MNRAS*, 271, 355
- 1996, *MNRAS*, 280, 130
- 1998, *MNRAS*, 296, 856
- Adelman, S. J. 1999, *MNRAS*, 310, 146

- Adelman, S. J., Bolcal, C., Kocer, D., & Hill, G. 1991, *MNRAS*, 252, 329
- Adelman, S. J. & Nasson, M. A. 1980, *PASP*, 92, 346
- Adelman, S. J. & Philip, A. G. D. 1992, *PASP*, 104, 316
- . 1994, *PASP*, 106, 1239
- Adelman, S. J. & Pintado, O. I. 1997, *A&AS*, 125, 219
- Andrillat, Y., Jaschek, C., & Jaschek, M. 1995, *A&A*, 299, 493
- Barklem, P. S., Piskunov, N., & O'Mara, B. J. 2000a, *A&AS*, 142, 467
- . 2000b, *A&A*, 355, L5
- Bohlender, D. A. & Landstreet, J. D. 1990, *MNRAS*, 247, 606
- Burbidge, E. M. & Burbidge, G. R. 1956, *ApJ*, 124, 116
- Caliskan, H. & Adelman, S. J. 1997, *MNRAS*, 288, 501
- Canuto, V. M. & Mazzitelli, I. 1991, *ApJ*, 370, 295
- Chernyshova, I. V., Andrievsky, S. M., Kovtyukh, V. V., & Mkrtichian, D. E. 1998, *Contrib. Astron. Obs. Skalnaté Pleso*, 27, 332
- Faraggiana, R. & Bonifacio, P. 1999, *A&A*, 349, 521
- Faraggiana, R., Gerbaldi, M., & Böhm, C. 1990, *A&A*, 235, 311
- Gelbmann, M., Kupka, F., Weiss, W. W., & Mathys, G. 1997, *A&A*, 319, 630
- Gray, R. O. 1988, *AJ*, 95, 220
- Gray, R. O. 1991, in *Precision Photometry*, ed. A. G. Davis Philip, A. R. Uppgren, & K. Janes (Schenectady, N.Y.: L. Davis Press), 309
- Gray, R. O. 1997, in *The Third Conference on Faint Blue Stars*, ed. A. G. Davis Philip, J. W. Liefert, R. A. Saffer, & D. S. Hayes (L. Davis Press), 237
- Gray, R. O. & Garrison, R. F. 1987, *ApJS*, 65, 581
- Grevesse, N., Noels, A., & Sauval, A. J. 1996, in *ASP Conf. Ser. 99: Cosmic Abundances*, 117
- Hauck, B. & Slettebak, A. 1983, *A&A*, 127, 231
- Heiter, U. 2000, PhD thesis, Univ. of Vienna, Austria, available as postscript file at <http://ams.astro.univie.ac.at/~heiter/thesis/thesis.ps.gz>
- Heiter, U., Kupka, F., Paunzen, E., Weiss, W., & Gelbmann, M. 1998, *A&A*, 335, 1009
- Heiter, U., Weiss, W. W., & Paunzen, E. 2001, *A&A*, in press (this volume)
- Iliev, I. K. & Barzova, I. S. 1996, in *Model Atmospheres and Spectrum Synthesis*, ed. S. J. Adelman, F. Kupka, & W. W. Weiss, 200
- Kamp, I., Iliev, I. K., Paunzen, E., et al. 2001, *A&A*, in press
- Kupka, F., Piskunov, N. E., Ryabchikova, T. A., Stempels, H. C., & Weiss, W. W. 1999, *A&AS*, 138, 119
- Kupka, F., Ryabchikova, T. A., Weiss, W. W., et al. 1996, *A&A*, 308, 886
- Kurucz, R. L. 1993a, CD-ROM 13, SAO
- . 1993b, CD-ROM 3 and 4, SAO
- Martinez, P., Koen, C., Handler, G., & Paunzen, E. 1998, *MNRAS*, 301, 1099
- Mashonkina, L. I., Shimanskaya, N. N., & Shimansky, V. V. 1996, *Odessa Astronomical Publications*, 9, 78
- Napiwotzky, R., Schönberner, D., & Wenske, V. 1993, *A&A*, 268, 653
- North, P., Berthet, S., & Lanz, T. 1994a, *A&A*, 281, 775
- . 1994b, *A&AS*, 103, 321
- Paunzen, E. 2000, PhD thesis, Univ. of Vienna, Austria, available on request from the author
- Paunzen, E., Andrievsky, S. M., Chernyshova, I. V., et al. 1999a, *A&A*, 351, 981
- Paunzen, E. & Gray, R. O. 1997, *A&AS*, 126, 407
- Paunzen, E., Heiter, U., Handler, G., et al. 1998, *A&A*, 329, 155
- Paunzen, E., Kamp, I., Iliev, I. K., et al. 1999b, *A&A*, 345, 597
- Piskunov, N. E. 1992, in *Stellar magnetism*, Nauka, St. Petersburg, 92
- Piskunov, N. E., Kupka, F., Ryabchikova, T. A., Weiss, W. W., & Jeffery, C. S. 1995, *A&AS*, 112, 525
- Renson, P., Gerbaldi, M., & Catalano, F. A. 1991, *A&AS*, 89, 429
- Smith, K. C. 1994, *A&A*, 291, 521
- Snedden, C., Gratton, R. G., & Crocker, D. A. 1991, *A&A*, 328, 349
- Solano, E. & Paunzen, E. 1998, *A&A*, 331, 633
- Solano, E., Paunzen, E., Pintado, O. I., & Varela, J. 2001, *A&A*, 374, 957
- Stürenburg, S. 1993, *A&A*, 277, 139
- Uesugi, A. & Fukuda, I. 1982, *Revised Catalogue of Stellar Rotational Velocities* (Kyoto: Department of Astronomy, Kyoto Univ.)
- Valenti, J. A. & Piskunov, N. 1996, *A&AS*, 118, 595
- van Winckel, H., Mathias, J., & Waelkens, C. 1992, *Nature*, 356, 500
- Varenne, O. & Monier, R. 1999, *A&A*, 351, 247
- Venn, K. A. & Lambert, D. L. 1990, *ApJ*, 363, 234
- Willmarth, D. & Barnes, J. 1994, *A User's Guide to Reducing Echelle Spectra with IRAF, NOAO*